Japanese Journal of Applied Physics
Vol. 47, No. 1, 2008, pp. 371–382

Theoretical Study of Nonequilibrium Electron Transport and Charge Distribution in a Three-Site Quantum Wire

Yangdong ZHENG, Hiroshi MIZUTA[1], and Shunri ODA*

Quantum Nanoelectronics Research Center and Department of Physical Electronics, Tokyo Institute of Technology, 2-12-1 O-okayama, Meguro-ku, Tokyo 152-8552, Japan
[1]*School of Electronics and Computer Science, Southampton University, Highfield, Southampton Hampshire SO17 1BJ, U.K.*

(Received July 13, 2007; accepted October 21, 2007; published online January 18, 2008)

We derive the nonequilibrium transport property formulas for a three-site quantum wire model using Keldysh formalism. Some rigorous formulas in the case of noninteraction are provided for direct calculations. On the basis of the numerical calculations, we investigate the differential and total conductances, transport current, and on-site electronic charges of a wire in some special cases. For a uniform-ingredient wire, if the temperature $T = 0\,\mathrm{K}$, it shows that, when site–site couplings in the wire are stronger than wire–electrode couplings, resonant tunneling transport takes place and the phenomenon of conductance quantization can be easily observed. In the opposite case, these quantum effects on transport disappear gradually with the increase in the strength of wire–electrode couplings. We also discuss the charge distributions in the three sites of the wire and the characteristics of the charge barrier (Schottky barrier) regardless of Coulomb interaction. If $T > 0\,\mathrm{K}$, all the line shapes of the transport properties become smoother than those at $T = 0\,\mathrm{K}$ owing to thermal fluctuations. For a wire containing impurities, the line shapes of the transport properties change because of the change of system electronic states.
[DOI: 10.1143/JJAP.47.371]

KEYWORDS: quantum wire, nonequilibrium electron transport, resonant tunneling, conductance quantization, charge distribution

1. Introduction

With advantage of top-down and bottom-up fabrication techniques for nanometer- scale structures, it becomes possible to fabricate quantum wires with diameters of the order of Fermi wavelength, and to experimentally study quantum transport properties through them.[1–5] In order to understand the experimental results, furthermore, to predict transport properties for applications in future nanodevice designs, various theoretical approaches[6,7] as well as simulation technologies[8–10] have been developed so far. In this paper, we present some theoretical formulas and numerical results for nonequilibrium transport properties, using the simplest model of a three-site quantum wire, in which each site has a single level.

Nonequilibrium electron transport and electronic charge distribution are the central problems of a mesoscopic system. In this study, the rigorous formulas of differential and total conductance, transport current and charge distributions for the three-site quantum wire model are derived on the basis of the nonequilibrium transport theory (Keldysh formalism). From these formulas, the relevance between the transport properties and the parameters in the Hamiltonian, as well as the temperature dependence of the transport properties will be expressed clearly and can be investigated in detail. Specifically, in the present study we concentrate on a noninteracting case for simplicity. The effects of interaction within a Hartree–Fock approximation level can be included in a straightforward manner. We report the results of numerical calculation using the formulas mentioned above, with respect to nonequilibrium electron transport and on-site charge distributions of the wire in some special cases, particularly focusing on resonant tunneling transport and conductance quantization phenomena as well as the characteristics of the charge barrier (Schottky barrier). The finite temperature case is also investigated. It is reasonable to consider that the results of our study are applicable to the complicated case of real quantum wires, which are probably longer, thicker, and containing larger numbers of atoms (sites) having multiple levels. On the other hand, the theoretical formulas described here also can be expanded in numerical calculations or first-principle simulations for real quantum wires.

The paper is organized as follows, in §2 we describe the three-site quantum wire model, corresponding Hamiltonian, and parameters appearing in the Hamiltonian. The brief description of nonequilibrium Keldysh formalism and the concise derivations for transport properties formulas of the three-site quantum wire will be given in §3. Section 4 is devoted to our present numerical results calculated from these formulas and their interpretations. Finally, we summarize our results and have a discussion in §5.

2. Model

We consider a one-dimensional quantum wire with three lattice sites that are mutually coupled by tunneling barriers. They are combined with two external electrodes as shown in Fig. 1.

The tight-binding Hamiltonian of such a system is described by eq. (1), which consists of four parts, the energy of electrons in the left and right electrodes, the on-site energy of wire sites, the coupling energy between sites in the wire, and the tunneling energy between the wire and the electrodes. Here, we ignored interaction terms. In the Hamiltonian, $\hat{\boldsymbol{c}}^{+}_{k\sigma,\alpha}$ and $\hat{\boldsymbol{c}}_{k\sigma,\alpha}$ ($\alpha = \mathrm{L}$ or R) denote creation and annihilation operators of an electron with the wave vector k and spin σ within L or R one-dimension perfect crystalline electrodes. The same operators of an electron within the i-th site of the center wire are denoted by $\hat{\boldsymbol{d}}^{+}_{i\sigma}$ and $\hat{\boldsymbol{d}}_{i\sigma}$. $\varepsilon_{k\sigma,\alpha}$ and $\varepsilon_{i\sigma}$ are the on-site energies in the electrodes and wire region, respectively. The transfer integrals between the nearest-neighbor sites are $t_{i,j\sigma}$. The sites labeled 1 and 3 are connected to the left and right electrodes, respectively, and $V_{\alpha,k\sigma}$ denote the tunnel combination integrals between those boundary sites and the

*E-mail address: soda@pe.titech.ac.jp

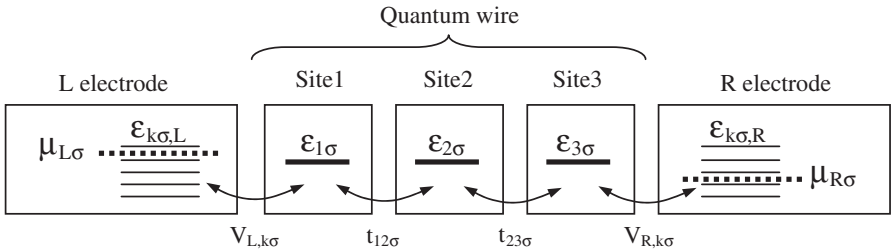

Fig. 1. Model of three-site quantum wire combined with two external electrodes. $\varepsilon_{k\sigma,\alpha}$ (α = L or R) and $\varepsilon_{i\sigma}$ are on-site energies in the electrodes and wire region, respectively. Transfer integrals between nearest-neighbor sites are $t_{i,j\sigma}$, and tunnel combination integrals between the wire and the electrodes are $V_{\alpha,k\sigma}$. μ_L and μ_R denote electrochemical potentials of the left and right electrodes, respectively.

electrodes. When the bias voltage $-V$ is applied to the wire, it can be regarded as the electrochemical potentials μ_L and μ_R associated with the left and right electrode, respectively ($eV = \mu_L - \mu_R$). We assume that the electrodes are electric reservoirs, the capacities of which are sufficiently large that μ_L and μ_R are not perturbed by transport current. In the case of $\mu_L > \mu_R$, electrons will flow from the left electrode to the right electrode.

$$\begin{aligned}\hat{\boldsymbol{H}} &= \hat{\boldsymbol{H}}_{\mathrm{ed}} + \hat{\boldsymbol{H}}_{\mathrm{wire}} + \hat{\boldsymbol{H}}_{\mathrm{wt}} + \hat{\boldsymbol{H}}_{\mathrm{ewt}} \\ &= \sum_{k\sigma}(\varepsilon_{k\sigma,\mathrm{L}}\hat{\boldsymbol{c}}^{+}_{k\sigma,\mathrm{L}}\hat{\boldsymbol{c}}_{k\sigma,\mathrm{L}} + \varepsilon_{k\sigma,\mathrm{R}}\hat{\boldsymbol{c}}^{+}_{k\sigma,\mathrm{R}}\hat{\boldsymbol{c}}_{k\sigma,\mathrm{R}}) + \sum_{\sigma}(\varepsilon_{1\sigma}\hat{\boldsymbol{d}}^{+}_{1\sigma}\hat{\boldsymbol{d}}_{1\sigma} + \varepsilon_{2\sigma}\hat{\boldsymbol{d}}^{+}_{2\sigma}\hat{\boldsymbol{d}}_{2\sigma} + \varepsilon_{3\sigma}\hat{\boldsymbol{d}}^{+}_{3\sigma}\hat{\boldsymbol{d}}_{3\sigma}) \\ &\quad + \sum_{\sigma}(t_{12\sigma}\hat{\boldsymbol{d}}^{+}_{1\sigma}\hat{\boldsymbol{d}}_{2\sigma} + t^{*}_{12\sigma}\hat{\boldsymbol{d}}^{+}_{2\sigma}\hat{\boldsymbol{d}}_{1\sigma} + t_{23\sigma}\hat{\boldsymbol{d}}^{+}_{2\sigma}\hat{\boldsymbol{d}}_{3\sigma} + t^{*}_{23\sigma}\hat{\boldsymbol{d}}^{+}_{3\sigma}\hat{\boldsymbol{d}}_{2\sigma}) \\ &\quad + \sum_{k\sigma}(V_{\mathrm{L},k\sigma}\hat{\boldsymbol{c}}^{+}_{k\sigma,\mathrm{L}}\hat{\boldsymbol{d}}_{1\sigma} + V^{*}_{\mathrm{L},k\sigma}\hat{\boldsymbol{d}}^{+}_{1\sigma}\hat{\boldsymbol{c}}_{k\sigma,\mathrm{L}}) + \sum_{k\sigma}(V_{\mathrm{R},k\sigma}\hat{\boldsymbol{c}}^{+}_{k\sigma,\mathrm{R}}\hat{\boldsymbol{d}}_{3\sigma} + V^{*}_{\mathrm{R},k\sigma}\hat{\boldsymbol{d}}^{+}_{3\sigma}\hat{\boldsymbol{c}}_{k\sigma,\mathrm{R}})\end{aligned} \tag{1}$$

3. Formulation

3.1 Nonequilibrium Keldysh formalism

We introduce Keldysh Green's function to solve the nonequilibrium transport problem in our study. The Keldysh formalism can be briefly described as follows. For a nonequilibrium problem, it is necessary to define how the system is perturbed from its equilibrium state, and to relate its nonequilibrium transport properties, e.g., steady current, to the electrochemical potentials μ_L and μ_R, which represent the local equilibrium of the electrodes, or the unperturbed Fermi distribution functions f_{μ_L} ($\varepsilon_{k\sigma}$) and f_{μ_R} ($\varepsilon_{k\sigma}$) in the electrodes. We consider a system consisting of three regions, a left electrode, a right electrode and an intermediate wire, that are uncoupled and each of which maintains its noninteraction thermal equilibrium at $t = -\infty$, then turn on the perturbation coupling $e^{\delta t}\hat{\boldsymbol{H}}_{\mathrm{ewt}}$ [$\hat{\boldsymbol{H}}_{\mathrm{ewt}}$ is the tunnel transfer term between the wire and electrodes in eq. (1)] adiabatically with the route $t = -\infty \to 0 \to +\infty \to -\infty$ (Keldysh contour).[11–13] In accordance with the quantum statistical theory,[14,15] any nonequilibrium observable physical quantity at time t can be expressed exactly as a statistical average shown as

$$\begin{aligned}\langle \boldsymbol{O}(t)\rangle &= \mathrm{Tr}[\boldsymbol{\rho}_{\mathrm{S}}(t)\boldsymbol{O}_{\mathrm{S}}] = \mathrm{Tr}[\boldsymbol{\rho}_{\mathrm{I}}(-\infty)\boldsymbol{U}(-\infty,+\infty)\boldsymbol{U}(+\infty,t)\boldsymbol{O}_{\mathrm{I}}(t)\boldsymbol{U}(t,-\infty)] \\ &= \sum_{n=0}^{\infty}\sum_{m=0}^{\infty}\frac{i^n}{n!}\frac{(-i)^m}{m!}\int_{-\infty}^{+\infty}dt'_1\cdots dt'_n\int_{-\infty}^{+\infty}dt_1\cdots dt_m\,\mathrm{Tr}\{[\tilde{\boldsymbol{T}}\boldsymbol{H}_{\mathrm{TI}}(t'_1)\cdots\boldsymbol{H}_{\mathrm{TI}}(t'_n)][\boldsymbol{T}\boldsymbol{H}_{\mathrm{TI}}(t_1)\cdots\boldsymbol{H}_{\mathrm{TI}}(t_m)\boldsymbol{O}_{\mathrm{I}}(t)]\},\end{aligned} \tag{2}$$

where $\boldsymbol{O}$ is an observable physical quantity operator, $\boldsymbol{U}$ is the time development operator, $\boldsymbol{\rho}$ is a statistical density matrix, and the subscripts S and I indicate Schrödinger and interaction representations of the operators, respectively. $\boldsymbol{H}_{\mathrm{T}}$ is the perturbation term in Hamiltonian, Tr[$\cdots$] is a trace operation symbol, and T and $\tilde{T}$ are the time-ordered and anti-time-ordered operators, respectively.

To carry out perturbation expansion by the Wick theorem in Feynman diagrams for eq. (2), one obtains four types of Keldysh Green's function shown in eqs. (3a)–(3d).[12,13] The corresponding Fourier transforms of the functions are defined in the parentheses. These functions can be used to calculate nonequilibrium observable physical quantities later.

$$G^{--}_{ij}(t,t_0) = -i\langle T\hat{\boldsymbol{c}}_i(t)\hat{\boldsymbol{c}}^{+}_j(t_0)\rangle \qquad \left(G^{--}_{ij}(\varepsilon) = \int_{-\infty}^{+\infty}G^{--}_{ij}(t,0)e^{-i\varepsilon t}\,dt\right) \tag{3a}$$

$$G^{++}_{ij}(t,t_0) = -i\langle \tilde{\boldsymbol{T}}\hat{\boldsymbol{c}}_i(t)\hat{\boldsymbol{c}}^{+}_j(t_0)\rangle \qquad \left(G^{++}_{ij}(\varepsilon) = \int_{-\infty}^{+\infty}G^{--}_{ij}(t,0)e^{-i\varepsilon t}\,dt\right) \tag{3b}$$

$$G^{>}_{ij}(t,t_0) = -i\langle \hat{\boldsymbol{c}}_i(t)\hat{\boldsymbol{c}}^{+}_j(t_0)\rangle \qquad \left(G^{>}_{ij}(\varepsilon) = \int_{-\infty}^{+\infty}G^{>}_{ij}(t,0)e^{-i\varepsilon t}\,dt\right) \tag{3c}$$

$$G^{<}_{ij}(t,t_0) = i\langle \hat{\boldsymbol{c}}^{+}_i(t)\hat{\boldsymbol{c}}_j(t_0)\rangle \qquad \left(G^{<}_{ij}(\varepsilon) = \int_{-\infty}^{+\infty}G^{<}_{ij}(t,0)e^{-i\varepsilon t}\,dt\right) \tag{3d}$$

where $\langle\cdots\rangle$ is the symbol of the statistical average.

It should be noted that four types of Keldysh Green's function are not independent of each other and have the relation of $G^{--} + G^{++} = G^{<} + G^{>}$. Keldysh Green's functions can be solved from the Dyson equation in the matrix form: $\boldsymbol{G}(\varepsilon) = \boldsymbol{g}(\varepsilon) + \boldsymbol{g}(\varepsilon)\boldsymbol{\Sigma}(\varepsilon)\boldsymbol{G}(\varepsilon)$. The matrix

$$\boldsymbol{G}(\varepsilon) = \begin{bmatrix} G_{ij}^{--}(\varepsilon) & G_{ij}^{<}(\varepsilon) \\ G_{ij}^{>}(\varepsilon) & G_{ij}^{++}(\varepsilon) \end{bmatrix}$$

contains four types of Keldysh Green's function, whereas the matrix

$$\boldsymbol{\Sigma}(\varepsilon) = \begin{bmatrix} \Sigma_{ij}^{--}(\varepsilon) & \Sigma_{ij}^{<}(\varepsilon) \\ \Sigma_{ij}^{>}(\varepsilon) & \Sigma_{ij}^{++}(\varepsilon) \end{bmatrix}$$

is a self-energy matrix, the elements of which represent the self-energy corresponding to those of the Keldysh Green's functions and have the relation of $\Sigma^{--} + \Sigma^{++} = -\Sigma^{<} - \Sigma^{>}$.

The matrix

$$\boldsymbol{g}(\varepsilon) = \begin{bmatrix} g_{ij}^{--}(\varepsilon) & g_{ij}^{<}(\varepsilon) \\ g_{ij}^{>}(\varepsilon) & g_{ij}^{++}(\varepsilon) \end{bmatrix}$$

contains unperturbed Keldysh Green's functions in the thermal equilibrium state when the wire and electrodes are not coupled at $t = -\infty$. In this case, the noninteracting statistical average $\langle \cdots \rangle_0$ can be expressed by the Fermi distribution function. When $i \neq j$, among the elements of $\boldsymbol{g}(\varepsilon)$, $g_{ij}(\varepsilon)$ is zero. The nonzero $g_{ij}(\varepsilon)$ can be calculated from their definitions shown in eqs. (4a)–(4d) when $i = j$,

$$g_{ii}^{--}(\varepsilon) = \frac{1 - f(\varepsilon_i - \varepsilon_F)}{\varepsilon - \varepsilon_i + i\delta} + \frac{f(\varepsilon_i - \varepsilon_F)}{\varepsilon - \varepsilon_i - i\delta}$$
$$= \frac{1}{\varepsilon - \varepsilon_i + i\delta} + 2\pi i f(\varepsilon_i - \varepsilon_F)\delta(\varepsilon - \varepsilon_i) \quad (4a)$$

$$g_{ii}^{++}(\varepsilon) = -\frac{f(\varepsilon_i - \varepsilon_F)}{\varepsilon - \varepsilon_i + i\delta} - \frac{1 - f(\varepsilon_i - \varepsilon_F)}{\varepsilon - \varepsilon_i - i\delta}$$
$$= -\frac{1}{\varepsilon - \varepsilon_i + i\delta} + 2\pi i[f(\varepsilon_i - \varepsilon_F) - 1]\delta(\varepsilon - \varepsilon_i) \quad (4b)$$

$$g_{ii}^{>}(\varepsilon) = -2\pi i[1 - f(\varepsilon_i - \varepsilon_F)]\delta(\varepsilon - \varepsilon_i)$$
$$= [1 - f(\varepsilon_i - \varepsilon_F)][g_{ij}^{r}(\varepsilon) - g_{ij}^{a}(\varepsilon)] \quad (4c)$$

$$g_{ii}^{<}(\varepsilon) = 2\pi i f(\varepsilon - \varepsilon_F)\delta(\varepsilon - \varepsilon_i)$$
$$= -f(\varepsilon_i - \varepsilon_F)[g_{ij}^{r}(\varepsilon) - g_{ij}^{a}(\varepsilon)] \quad (4d)$$

where ε_i and ε_F are the molecular orbit level and the Fermi level, respectively. δ represents an infinite small constant value, and $\delta(\varepsilon)$ is a δ function. The Fermi distribution function is given by

$$f(\varepsilon_i - \varepsilon_F) = \left[1 + \exp\left(\frac{\varepsilon_i - \varepsilon_F}{k_B T}\right)\right]^{-1}.$$

In particularly, it is convenient to introduce the transformation matrix

$$\boldsymbol{P} = \frac{1}{\sqrt{2}}\begin{bmatrix} 1 & 1 \\ -1 & 1 \end{bmatrix}$$

to transform the matrices in the Dyson equation into $\boldsymbol{G} = \boldsymbol{P}^{-1}\boldsymbol{G}\boldsymbol{P}$, $\boldsymbol{\Sigma} = \boldsymbol{P}^{-1}\boldsymbol{\Sigma}\boldsymbol{P}$, and $\boldsymbol{g} = \boldsymbol{P}^{-1}\boldsymbol{g}\boldsymbol{P}$.[15] Using new definitions of Green's functions, the Dyson equation becomes

$$\begin{bmatrix} 0 & G_{ij}^{a}(\varepsilon) \\ G_{ij}^{r}(\varepsilon) & F_{ij}(\varepsilon) \end{bmatrix} = \begin{bmatrix} 0 & g_{ij}^{a}(\varepsilon) \\ g_{ij}^{r}(\varepsilon) & F_{ij}^{0}(\varepsilon) \end{bmatrix} + \sum_{pq}\begin{bmatrix} 0 & g_{ip}^{a}(\varepsilon) \\ g_{ip}^{r}(\varepsilon) & F_{ip}^{0}(\varepsilon) \end{bmatrix}\begin{bmatrix} \Omega_{pq}(\varepsilon) & \Sigma_{pq}^{r}(\varepsilon) \\ \Sigma_{pq}^{a}(\varepsilon) & 0 \end{bmatrix}\begin{bmatrix} 0 & G_{qj}^{a}(\varepsilon) \\ G_{qj}^{r}(\varepsilon) & F_{qj}(\varepsilon) \end{bmatrix}, \quad (5)$$

where the retarded, advanced and F Green's functions in the matrices are defined by eqs. (6a)–(6c), respectively, and the retarded, advanced and F self-energies are given by $\Sigma^{r} = \Sigma^{--} + \Sigma^{<}$, $\Sigma^{a} = \Sigma^{--} + \Sigma^{>}$, and $\Omega = \Sigma^{--} + \Sigma^{++} = -\Sigma^{<} - \Sigma^{>}$, respectively.

$$G^{r} = G^{--} - G^{<}, \quad g^{r} = g^{--} - g^{<} \quad (6a)$$

$$G^{a} = G^{--} - G^{>}, \quad g^{a} = g^{--} - g^{>} \quad (6b)$$

$$F = G^{--} + G^{++} = G^{<} + G^{>}, \quad F^{0} = g^{--} + g^{++} = g^{<} + g^{>} \quad (6c)$$

On the other hand, the retarded and advanced Green's functions can also be defined by the well-known forms of $G_{ij}^{r}(t, t_0) = -i\theta(t - t_0)\langle \hat{\boldsymbol{c}}_i(t)\hat{\boldsymbol{c}}_j^{+}(t_0) + \hat{\boldsymbol{c}}_j^{+}(t_0)\hat{\boldsymbol{c}}_i(t)\rangle$ and $G_{ij}^{a}(t, t_0) = i\theta(t_0 - t)\langle \hat{\boldsymbol{c}}_i(t)\hat{\boldsymbol{c}}_j^{+}(t_0) + \hat{\boldsymbol{c}}_j^{+}(t_0)\hat{\boldsymbol{c}}_i(t)\rangle$.

Similar to eq. (4), in the thermal equilibrium state when the wire and electrodes are not coupled at $t = -\infty$, the retarded and advanced Green's functions are nonzero only when $i = j$ and can be calculated from their definitions shown as

$$g_{ij}^{r}(\varepsilon) = \frac{1}{\varepsilon - \varepsilon_i + i\delta} \quad (7a)$$

$$g_{ij}^{a}(\varepsilon) = \frac{1}{\varepsilon - \varepsilon_i - i\delta}. \quad (7b)$$

The F Green's function can be express by the Fermi distribution function in the thermal equilibrium state as follows.

$$F_{ij}^{0}(\varepsilon) = [1 - 2f(\varepsilon_i - \varepsilon_F)][g_{ij}^{r}(\varepsilon) - g_{ij}^{a}(\varepsilon)]$$
$$= -2\pi i[1 - 2f(\varepsilon - \varepsilon_F)]\delta(\varepsilon - \varepsilon_i) \quad (7c)$$

By expanding the Dyson equation of eq. (5), we obtain some useful formulas for the direct calculations of the retarded, advanced, and F Green's functions, as shown below.

$$\boldsymbol{G}^{r} = (\boldsymbol{1} - \boldsymbol{g}^{r}\boldsymbol{\Sigma}^{r})^{-1}\boldsymbol{g}^{r} \quad (8a)$$

$$\boldsymbol{G}^{a} = (\boldsymbol{1} - \boldsymbol{g}^{a}\boldsymbol{\Sigma}^{a})^{-1}\boldsymbol{g}^{a} \quad (8b)$$

$$\boldsymbol{F} = \boldsymbol{G}^{r}(\boldsymbol{g}^{r})^{-1}\boldsymbol{F}^{0}(\boldsymbol{g}^{a})^{-1}\boldsymbol{G}^{a} + \boldsymbol{G}^{r}\boldsymbol{\Omega}\boldsymbol{G}^{a} \quad (8c)$$

Reversely, the original Keldysh Green's functions also can be expressed by the retarded, advanced and F Green's functions as follows.

$$G^{--} = \frac{F + G^{r} + G^{a}}{2} \quad (9a)$$

$$G^{++} = \frac{F - G^{\mathrm{r}} - G^{\mathrm{a}}}{2} \tag{9b}$$

$$G^{<} = \frac{F - G^{\mathrm{r}} + G^{\mathrm{a}}}{2} \tag{9c}$$

$$G^{>} = \frac{F + G^{\mathrm{r}} - G^{\mathrm{a}}}{2} \tag{9d}$$

As indicated in the beginning of this section, nonequilibrium observable physical quantity can be expressed by Keldysh Green's functions shown above. With regard to transport properties, the single-spin current between the wire region and the left electrode is given by[16)]

$$\begin{aligned} I &= \frac{ie}{\hbar}\sum_{k\sigma,n}(V_{k\sigma-\mathrm{L},n\sigma}\langle\hat{\boldsymbol{c}}^{+}_{k\sigma,\mathrm{L}}(0)\hat{\boldsymbol{d}}_{n\sigma}(t)\rangle - V^{*}_{k\sigma-\mathrm{L},n\sigma}\langle\hat{\boldsymbol{d}}^{+}_{n\sigma}(0)\hat{\boldsymbol{c}}_{k\sigma,\mathrm{L}}(t)\rangle)|_{t=0} \\ &= \frac{e}{\hbar}\sum_{k\sigma,n}\int_{-\infty}^{+\infty}\frac{d\varepsilon}{2\pi}e^{-i\varepsilon t}[V_{\mathrm{L},k\sigma,n}G^{<}_{n,k\sigma-\mathrm{L}}(\varepsilon) - V^{*}_{\mathrm{L},k\sigma,n}G^{<}_{k\sigma-\mathrm{L},n}(\varepsilon)]|_{t=0} \\ &= \frac{e}{\hbar}\sum_{k\sigma,n}\int_{-\infty}^{+\infty}\frac{d\varepsilon}{2\pi}[V_{k\sigma-\mathrm{L},n\sigma}G^{<}_{n,k\sigma-\mathrm{L}}(\varepsilon) - V^{*}_{k\sigma-\mathrm{L},n\sigma}G^{<}_{k\sigma-\mathrm{L},n}(\varepsilon)]. \end{aligned} \tag{10}$$

The single-spin electron charge on the site n is given by

$$\begin{aligned} \rho_{n\sigma} &= e\langle\hat{\boldsymbol{d}}^{+}_{n\sigma}(0)\hat{\boldsymbol{d}}_{n\sigma}(t)\rangle|_{t=0} = e(-i)G^{<}_{n\sigma,n\sigma}(t,0)|_{t=0} \\ &= e(-i)\int_{-\infty}^{+\infty}\frac{d\varepsilon}{2\pi}e^{-i\varepsilon t}G^{<}_{n\sigma,n\sigma}(\varepsilon)|_{t=0} = e(-i)\frac{1}{2\pi}\int_{-\infty}^{+\infty}d\varepsilon\, G^{<}_{n\sigma,n\sigma}(\varepsilon). \end{aligned} \tag{11}$$

3.2 Transport property formulas

In this study, we assume the perturbed item of the Hamiltonian in eq. (1) as

$$\hat{\boldsymbol{H}}_{\mathrm{ewt}} = \sum_{k}(V_{\mathrm{L},k\sigma}\hat{\boldsymbol{c}}^{+}_{\mathrm{L},k\sigma}\hat{\boldsymbol{d}}_{1\sigma} + V^{*}_{\mathrm{L},k\sigma}\hat{\boldsymbol{d}}^{+}_{1\sigma}\hat{\boldsymbol{c}}_{\mathrm{L},k\sigma}) + \sum_{k}(V_{\mathrm{R},k\sigma}\hat{\boldsymbol{c}}^{+}_{\mathrm{R},k\sigma}\hat{\boldsymbol{d}}_{3\sigma} + V^{*}_{\mathrm{R},k\sigma}\hat{\boldsymbol{d}}^{+}_{3\sigma}\hat{\boldsymbol{c}}_{\mathrm{R},k\sigma}).$$

Thus, the self-energy matrix $\boldsymbol{\Sigma}(\varepsilon)$ in the Dyson equation is proved as the expression of eq. (12):

$$\begin{aligned} \boldsymbol{\Sigma}_{pq}(\varepsilon) &= \begin{bmatrix} \Sigma^{--}_{pq}(\varepsilon) & \Sigma^{<}_{pq}(\varepsilon) \\ \Sigma^{>}_{pq}(\varepsilon) & \Sigma^{++}_{pq}(\varepsilon) \end{bmatrix} \\ &= \sum_{k\sigma}V^{*}_{\mathrm{L},k\sigma}\delta_{p,1\sigma}\delta_{q,k\sigma-\mathrm{L}}\begin{bmatrix} 1 & 0 \\ 0 & -1 \end{bmatrix} + \sum_{k\sigma}V_{\mathrm{L},k\sigma}\delta_{p,k\sigma-\mathrm{L}}\delta_{q,1\sigma}\begin{bmatrix} 1 & 0 \\ 0 & -1 \end{bmatrix} \\ &\quad + \sum_{k\sigma}V^{*}_{\mathrm{R},k\sigma}\delta_{p,N\sigma}\delta_{q,k\sigma-\mathrm{R}}\begin{bmatrix} 1 & 0 \\ 0 & -1 \end{bmatrix} + \sum_{k\sigma}V_{\mathrm{R},k\sigma}\delta_{p,k\sigma-\mathrm{R}}\delta_{q,N\sigma}\begin{bmatrix} 1 & 0 \\ 0 & -1 \end{bmatrix}. \end{aligned} \tag{12}$$

The corresponding retarded, advanced, and F self-energies are given by eqs. (13a)–(13c), respectively.

$$\Sigma^{\mathrm{r}}_{pq}(\varepsilon) = \sum_{k\sigma}V^{*}_{\mathrm{L},k\sigma}\delta_{p,1\sigma}\delta_{q,k\sigma-\mathrm{L}} + \sum_{k\sigma}V_{\mathrm{L},k\sigma}\delta_{p,k\sigma-\mathrm{L}}\delta_{q,1\sigma} + \sum_{k\sigma}V^{*}_{\mathrm{R},k\sigma}\delta_{p,3\sigma}\delta_{q,k\sigma-\mathrm{R}} + \sum_{k\sigma}V_{\mathrm{R},k\sigma}\delta_{p,k\sigma-\mathrm{R}}\delta_{q,3\sigma} \tag{13a}$$

$$\Sigma^{\mathrm{a}}_{pq}(\varepsilon) = \sum_{k\sigma}V^{*}_{\mathrm{L},k\sigma}\delta_{p,1\sigma}\delta_{q,k\sigma-\mathrm{L}} + \sum_{k\sigma}V_{\mathrm{L},k\sigma}\delta_{p,k\sigma-\mathrm{L}}\delta_{q,1\sigma} + \sum_{k\sigma}V^{*}_{\mathrm{R},k\sigma}\delta_{p,3\sigma}\delta_{q,k\sigma-\mathrm{R}} + \sum_{k\sigma}V_{\mathrm{R},k\sigma}\delta_{p,k\sigma-\mathrm{R}}\delta_{q,3\sigma} \tag{13b}$$

$$\Omega_{pq}(\varepsilon) = 0 \tag{13c}$$

Then eq. (8c) is reduced to

$$\boldsymbol{F} = \boldsymbol{G}^{\mathrm{r}}(\boldsymbol{g}^{\mathrm{r}})^{-1}\boldsymbol{F}^{0}(\boldsymbol{g}^{\mathrm{a}})^{-1}\boldsymbol{G}^{\mathrm{a}}. \tag{14}$$

Generally, the retarded and advanced Green's functions of the system can be obtained from eqs. (8a) and (8b), if we know the uncoupling initial Green's functions and self-energy matrices. Specifically, in the noninteracting case, they can also be derived from simultaneous motion equations. In this study, we use the latter method and deduce them for the three-site quantum wire system.

On the basis of the simultaneous motion, we obtain a matrix equation for the elements of retarded (advanced) Green's functions between the sites in the wire as follows:

$$\begin{bmatrix} \varepsilon - \varepsilon_{1\sigma} \pm i\Gamma^{\mathrm{r}}_{\mathrm{L}\sigma} & -t_{12\sigma} & 0 \\ -t^{*}_{12\sigma} & \varepsilon - \varepsilon_{2\sigma} \pm i\delta & -t_{23\sigma} \\ 0 & -t^{*}_{23\sigma} & \varepsilon - \varepsilon_{3\sigma} \pm i\Gamma^{\mathrm{r}}_{\mathrm{R}\sigma} \end{bmatrix}\begin{bmatrix} G^{\mathrm{r(a)}}_{1\sigma,1\sigma}(\varepsilon) & G^{\mathrm{r(a)}}_{1\sigma,2\sigma}(\varepsilon) & G^{\mathrm{r(a)}}_{1\sigma,3\sigma}(\varepsilon) \\ G^{\mathrm{r(a)}}_{2\sigma,1\sigma}(\varepsilon) & G^{\mathrm{r(a)}}_{2\sigma,2\sigma}(\varepsilon) & G^{\mathrm{r(a)}}_{2\sigma,3\sigma}(\varepsilon) \\ G^{\mathrm{r(a)}}_{3\sigma,1\sigma}(\varepsilon) & G^{\mathrm{r(a)}}_{3\sigma,2\sigma}(\varepsilon) & G^{\mathrm{r(a)}}_{3\sigma,3\sigma}(\varepsilon) \end{bmatrix} = \begin{bmatrix} 1 & 0 & 0 \\ 0 & 1 & 0 \\ 0 & 0 & 1 \end{bmatrix}, \tag{15}$$

where $i\Gamma^{\mathrm{r}}_{\mathrm{L(R)}\sigma}(\varepsilon) = i\pi\nu_{\mathrm{L(R)},\sigma}(\varepsilon)|V_{\mathrm{L(R)},k\sigma}|^2$ represent the self-energies of the site in the wire owing to the combination of the electrodes, where $\nu_{\mathrm{L(R)},\sigma}(\varepsilon)$ are the density-of-states (DOS) in the electrodes.

For the solution of the matrix equation above, the elements of retarded (advanced) Green's functions between the sites in the wire are given by

$$G^{\mathrm{r(a)}}_{1\sigma,1\sigma}(\varepsilon)=\frac{(\varepsilon-\varepsilon_{2\sigma}\pm i\delta)(\varepsilon-\varepsilon_{3\sigma}\pm i\Gamma^{\mathrm{r}}_{\mathrm{R}\sigma})-|t_{23\sigma}|^2}{B^{\mathrm{r(a)}}_{\sigma}} \tag{16a}$$

$$G^{\mathrm{r(a)}}_{1\sigma,2\sigma}(\varepsilon)=\frac{(\varepsilon-\varepsilon_{3\sigma}\pm i\Gamma^{\mathrm{r}}_{\mathrm{R}\sigma})t_{12\sigma}}{B^{\mathrm{r(a)}}_{\sigma}} \tag{16b}$$

$$G^{\mathrm{r(a)}}_{1\sigma,3\sigma}(\varepsilon)=\frac{t_{12\sigma}t_{23\sigma}}{B^{\mathrm{r(a)}}_{\sigma}} \tag{16c}$$

$$G^{\mathrm{r(a)}}_{2\sigma,2\sigma}(\varepsilon)=\frac{(\varepsilon-\varepsilon_{1\sigma}\pm i\Gamma^{\mathrm{r}}_{\mathrm{L}\sigma})(\varepsilon-\varepsilon_{3\sigma}\pm i\Gamma^{\mathrm{r}}_{\mathrm{R}\sigma})}{B^{\mathrm{r(a)}}_{\sigma}} \tag{16d}$$

$$G^{\mathrm{r(a)}}_{2\sigma,1\sigma}(\varepsilon)=\frac{(\varepsilon-\varepsilon_{3\sigma}\pm i\Gamma^{\mathrm{r}}_{\mathrm{R}\sigma})t^{*}_{12\sigma}}{B^{\mathrm{r(a)}}_{\sigma}} \tag{16e}$$

$$G^{\mathrm{r(a)}}_{2\sigma,3\sigma}(\varepsilon)=\frac{(\varepsilon-\varepsilon_{1\sigma}\pm i\Gamma^{\mathrm{r}}_{\mathrm{L}\sigma})t_{23\sigma}}{B^{\mathrm{r(a)}}_{\sigma}} \tag{16f}$$

$$G^{\mathrm{r(a)}}_{3\sigma,3\sigma}(\varepsilon)=\frac{(\varepsilon-\varepsilon_{1\sigma}\pm i\Gamma^{\mathrm{r}}_{\mathrm{L}\sigma})(\varepsilon-\varepsilon_{2\sigma}\pm i\delta)-|t_{12\sigma}|^2}{B^{\mathrm{r(a)}}_{\sigma}} \tag{16g}$$

$$G^{\mathrm{r(a)}}_{3\sigma,1\sigma}(\varepsilon)=\frac{t^{*}_{12\sigma}t^{*}_{23\sigma}}{B^{\mathrm{r(a)}}_{\sigma}} \tag{16h}$$

$$G^{\mathrm{r(a)}}_{3\sigma,2\sigma}(\varepsilon)=\frac{(\varepsilon-\varepsilon_{1\sigma}\pm i\Gamma^{\mathrm{r}}_{\mathrm{L}\sigma})t^{*}_{23\sigma}}{B^{\mathrm{r(a)}}_{\sigma}}. \tag{16i}$$

Here, the variable $B^{\mathrm{r(a)}}_{\sigma}$ is given by

$$\begin{aligned}B^{\mathrm{r(a)}}_{\sigma}=&(\varepsilon-\varepsilon_{1\sigma}\pm i\Gamma^{\mathrm{r}}_{\mathrm{L}\sigma})(\varepsilon-\varepsilon_{2\sigma}\pm i\delta)(\varepsilon-\varepsilon_{3\sigma}\pm i\Gamma^{\mathrm{r}}_{\mathrm{R}\sigma})\\&-(\varepsilon-\varepsilon_{1\sigma}\pm i\Gamma^{\mathrm{r}}_{\mathrm{L}\sigma})|t_{23\sigma}|^2\\&-(\varepsilon-\varepsilon_{3\sigma}\pm i\Gamma^{\mathrm{r}}_{\mathrm{R}\sigma})|t_{12\sigma}|^2.\end{aligned} \tag{16j}$$

The upper or lower sign (+ or −) denotes the retarded or advanced Green's functions, respectively.

The retarded (advanced) Green's functions between the $n\sigma$ site in the wire and the $k\sigma$ electronic state in the left and right electrodes are solved from the motion equations or the matrix equations (17a) and (17b). They are shown in eqs. (18a)–(18d):

$$\begin{bmatrix}\varepsilon-\varepsilon_{1\sigma}\pm i\Gamma^{\mathrm{r}}_{\mathrm{L}\sigma} & -t_{12\sigma} & 0\\ -t^{*}_{12\sigma} & \varepsilon-\varepsilon_{2\sigma}\pm i\delta & -t_{23\sigma}\\ 0 & -t^{*}_{23\sigma} & \varepsilon-\varepsilon_{3\sigma}\pm i\Gamma^{\mathrm{r}}_{\mathrm{R}\sigma}\end{bmatrix}\begin{bmatrix}G^{\mathrm{r(a)}}_{1\sigma,,k\sigma-\mathrm{L}}(\varepsilon)\\ G^{\mathrm{r(a)}}_{2\sigma,,k\sigma-\mathrm{L}}(\varepsilon)\\ G^{\mathrm{r(a)}}_{3\sigma,,k\sigma-\mathrm{L}}(\varepsilon)\end{bmatrix}=g^{\mathrm{r(a)}}_{k\sigma-\mathrm{L},k\sigma-\mathrm{L}}V^{*}_{\mathrm{L},k\sigma}\begin{bmatrix}1\\0\\0\end{bmatrix} \tag{17a}$$

$$\begin{bmatrix}\varepsilon-\varepsilon_{1\sigma}\pm i\Gamma^{\mathrm{r}}_{\mathrm{L}\sigma} & -t_{12\sigma} & 0\\ -t^{*}_{12\sigma} & \varepsilon-\varepsilon_{2\sigma}\pm i\delta & -t_{23\sigma}\\ 0 & -t^{*}_{23\sigma} & \varepsilon-\varepsilon_{3\sigma}\pm i\Gamma^{\mathrm{r}}_{\mathrm{R}\sigma}\end{bmatrix}\begin{bmatrix}G^{\mathrm{r(a)}}_{1\sigma,,k\sigma-\mathrm{R}}(\varepsilon)\\ G^{\mathrm{r(a)}}_{2\sigma,,k\sigma-\mathrm{R}}(\varepsilon)\\ G^{\mathrm{r(a)}}_{3\sigma,,k\sigma-\mathrm{R}}(\varepsilon)\end{bmatrix}=g^{\mathrm{r(a)}}_{k\sigma-\mathrm{R},k\sigma-\mathrm{R}}V^{*}_{\mathrm{R},k\sigma}\begin{bmatrix}0\\0\\1\end{bmatrix} \tag{17b}$$

$$G^{\mathrm{r(a)}}_{k\sigma-\mathrm{L},n\sigma}=g^{\mathrm{r(a)}}_{k\sigma-\mathrm{L},k\sigma-\mathrm{L}}V_{\mathrm{L},k\sigma}G^{\mathrm{r(a)}}_{1\sigma,n\sigma} \tag{18a}$$

$$G^{\mathrm{r(a)}}_{k\sigma-\mathrm{R},n\sigma}=g^{\mathrm{r(a)}}_{k\sigma-\mathrm{R},k\sigma-\mathrm{R}}V_{\mathrm{R},k\sigma}G^{\mathrm{r(a)}}_{N\sigma,n\sigma} \tag{18b}$$

$$G^{\mathrm{r(a)}}_{n\sigma,k\sigma-\mathrm{L}}=g^{\mathrm{r(a)}}_{k\sigma-\mathrm{L},k\sigma-\mathrm{L}}V^{*}_{\mathrm{L},k\sigma}G^{\mathrm{r(a)}}_{n\sigma,1\sigma} \tag{18c}$$

$$G^{\mathrm{r(a)}}_{n\sigma,k\sigma-\mathrm{R}}=g^{\mathrm{r(a)}}_{k\sigma-\mathrm{R},k\sigma-\mathrm{R}}V^{*}_{k\sigma-\mathrm{R}}G^{\mathrm{r(a)}}_{n\sigma,N\sigma}, \tag{18d}$$

where $n=1,2,3$, $N=3$.

$$g^{\mathrm{r(a)}}_{k\sigma-\mathrm{L(R)},k\sigma-\mathrm{L(R)}}=\frac{1}{\varepsilon-\varepsilon_{k\sigma-\mathrm{L(R)}}\pm i\delta}$$

are Green's functions in the thermal equilibrium state when the wire and electrodes are not coupled at $t=-\infty$.

Similarly, the retarded (advanced) Green's functions between the $k_1\sigma$ and $k_2\sigma$ electronic states in the left and right electrodes can be directly obtained from the motion equations and given by

$$G^{\mathrm{r(a)}}_{k_1\sigma-\mathrm{L},k_2\sigma-\mathrm{L}}=g^{\mathrm{r(a)}}_{k_1\sigma-\mathrm{L},k_1\sigma-\mathrm{L}}\delta(k_1,k_2)+g^{\mathrm{r(a)}}_{k_1\sigma-\mathrm{L},k_1\sigma-\mathrm{L}}V_{\mathrm{L},k_1\sigma}G^{\mathrm{r(a)}}_{1\sigma,k_2\sigma-\mathrm{L}} \tag{19a}$$

$$G^{\mathrm{r(a)}}_{k_1\sigma-\mathrm{R},k_2\sigma-\mathrm{L}}=g^{\mathrm{r(a)}}_{k_1\sigma-\mathrm{R},k_1\sigma-\mathrm{R}}V_{\mathrm{R},k_1\sigma}G^{\mathrm{r(a)}}_{N\sigma,k_2\sigma-\mathrm{L}} \tag{19b}$$

$$G^{\mathrm{r(a)}}_{k_1\sigma-\mathrm{L},k_2\sigma-\mathrm{R}}=g^{\mathrm{r(a)}}_{k_1\sigma-\mathrm{L},k_1\sigma-\mathrm{L}}V_{\mathrm{L},k_1\sigma}G^{\mathrm{r(a)}}_{1\sigma,k_2\sigma-\mathrm{R}} \tag{19c}$$

$$G^{\mathrm{r(a)}}_{k_1\sigma-\mathrm{R},k_2\sigma-\mathrm{R}}=g^{\mathrm{r(a)}}_{k_1\sigma-\mathrm{R},k_2\sigma-\mathrm{R}}\delta(k_1,k_2)+g^{\mathrm{r(a)}}_{k_1\sigma-\mathrm{R},k_2\sigma-\mathrm{R}}V_{\mathrm{R},k_1\sigma}G^{\mathrm{r(a)}}_{N\sigma,k_2\sigma-\mathrm{R}}. \tag{19d}$$

We next can use the retarded and advanced Green's functions to derive the F Green's functions by eq. (14). A part of the F Green's functions that will be applied in transport properties calculations are presented below.

As a result, the F Green's function between the 1σ site in the wire and the $k\sigma$ electronic state in the left electrodes are given by

$$\begin{aligned}F_{1\sigma,k\sigma-\mathrm{L}}=&(1-2f_{\mu_\mathrm{L}})V^{*}_{\mathrm{L},k\sigma}\{(g^{\mathrm{r}}_{k\sigma-\mathrm{L},k\sigma-\mathrm{L}}-g^{\mathrm{a}}_{k\sigma-\mathrm{L},k\sigma-\mathrm{L}})G^{\mathrm{r}}_{1\sigma,1\sigma}+2g^{\mathrm{a}}_{k\sigma-\mathrm{L},k\sigma-\mathrm{L}}[-i\Gamma^{\mathrm{r}}_{\mathrm{L}\sigma}]G^{\mathrm{r}}_{1\sigma,1\sigma}G^{\mathrm{a}}_{1\sigma,1\sigma}\}\\&+(1-2f_{\mu_\mathrm{R}})V^{*}_{\mathrm{L},k\sigma}\{2g^{\mathrm{a}}_{k\sigma-\mathrm{L},k\sigma-\mathrm{L}}[-i\Gamma^{\mathrm{r}}_{\mathrm{R}\sigma}]G^{\mathrm{r}}_{1\sigma,3\sigma}G^{\mathrm{a}}_{3\sigma,1\sigma}\}\end{aligned} \tag{20a}$$

$$\begin{aligned}F_{k\sigma-\mathrm{L},1\sigma}=&(1-2f_{\mu_\mathrm{L}})V_{\mathrm{L},k\sigma}\{(g^{\mathrm{r}}_{k\sigma-\mathrm{L},k\sigma-\mathrm{L}}-g^{\mathrm{a}}_{k\sigma-\mathrm{L},k\sigma-\mathrm{L}})G^{\mathrm{a}}_{1\sigma,1\sigma}+2g^{\mathrm{r}}_{k\sigma-\mathrm{L},k\sigma-\mathrm{L}}[-i\Gamma^{\mathrm{r}}_{\mathrm{L}\sigma}]G^{\mathrm{r}}_{1\sigma,1\sigma}G^{\mathrm{a}}_{1\sigma,1\sigma}\}\\&+(1-2f_{\mu_\mathrm{R}})V_{\mathrm{L},k\sigma}\{2g^{\mathrm{r}}_{k\sigma-\mathrm{L},k\sigma-\mathrm{L}}[-i\Gamma^{\mathrm{r}}_{\mathrm{R}\sigma}]G^{\mathrm{r}}_{1\sigma,3\sigma}G^{\mathrm{a}}_{3\sigma,1\sigma}\}.\end{aligned} \tag{20b}$$

The on-site (wire region) F Green's functions are given by

$$F_{1\sigma,1\sigma} = (1-2f_{\mu_L})[-2i\Gamma^r_{L\sigma}]G^r_{1\sigma,1\sigma}G^a_{1\sigma,1\sigma} + (1-2f_{\mu_R})[-2i\Gamma^r_{R\sigma}]G^r_{1\sigma,3\sigma}G^a_{3\sigma,1\sigma} \tag{21a}$$

$$F_{2\sigma,2\sigma} = (1-2f_{\mu_L})[-2i\Gamma^r_{L\sigma}]G^r_{2\sigma,1\sigma}G^a_{1\sigma,2\sigma} + (1-2f_{\mu_R})[-2i\Gamma^r_{R\sigma}]G^r_{2\sigma,3\sigma}G^a_{3\sigma,2\sigma} \tag{21b}$$

$$F_{3\sigma,3\sigma} = (1-2f_{\mu_L})[-2i\Gamma^r_{L\sigma}]G^r_{3\sigma,1\sigma}G^a_{1\sigma,3\sigma} + (1-2f_{\mu_R})[-2i\Gamma^r_{R\sigma}]G^r_{3\sigma,3\sigma}G^a_{3\sigma,3\sigma}. \tag{21c}$$

The four types of Keldysh Green's function can be recovered straightforwardly from the retarded, advanced, and F Green's functions as mentioned in §3.1. We only aim at lesser Green's functions $G^<$ concerning the transport properties.

As a result, the lesser Green's functions $G^<$ between the 1σ site in the wire and the $k\sigma$ electronic state in the left electrodes are given by

$$G^<_{1\sigma,k\sigma-L} = (1/2)[F_{1\sigma,k\sigma-L} - V^*_{L,k\sigma}(g^r_{k\sigma-L,k\sigma-L}G^r_{1\sigma,1\sigma} - g^a_{k\sigma-L,k\sigma-L}G^a_{1\sigma,1\sigma})] \tag{22a}$$

$$G^<_{k\sigma-L,1\sigma} = (1/2)[F_{k\sigma-L,1\sigma} - V_{L,k\sigma}(g^r_{k\sigma-L,k\sigma-L}G^r_{1\sigma,1\sigma} - g^a_{k\sigma-L,k\sigma-L}G^a_{1\sigma,1\sigma})]. \tag{22b}$$

If we suppose that $x_{1\sigma} = \varepsilon - \varepsilon_{1\sigma}, x_{2\sigma} = \varepsilon - \varepsilon_{2\sigma}, x_{3\sigma} = \varepsilon - \varepsilon_{3\sigma}$, the on-site (wire region) $G^<$ functions will be obtained as

$$G^<_{1\sigma,1\sigma} = 2i\frac{f_{\mu_L}\Gamma^r_{L\sigma}[(x_{2\sigma}x_{3\sigma} - |t_{23\sigma}|^2)^2 + (\Gamma^r_{R\sigma})^2x^2_{2\sigma}] + f_{\mu_R}\Gamma^r_{R\sigma}|t_{12\sigma}t_{23\sigma}|^2}{|B^r_\sigma|^2} \tag{23a}$$

$$G^<_{2\sigma,2\sigma} = 2i\frac{f_{\mu_L}\Gamma^r_{L\sigma}[x^2_{3\sigma} + (\Gamma^r_{R\sigma})^2]|t_{12\sigma}|^2 + f_{\mu_R}\Gamma^r_{R\sigma}[x^2_{1\sigma} + (\Gamma^r_{L\sigma})^2]|t_{23\sigma}|^2}{|B^r_\sigma|^2} \tag{23b}$$

$$G^<_{3\sigma,3\sigma} = 2i\frac{f_{\mu_L}\Gamma^r_{L\sigma}|t_{12\sigma}t_{23\sigma}|^2 + f_{\mu_R}\Gamma^r_{R\sigma}[(x_{1\sigma}x_{2\sigma} - |t_{12\sigma}|^2)^2 + (\Gamma^r_{L\sigma})^2x^2_{2\sigma}]}{|B^r_\sigma|^2}, \tag{23c}$$

where the Fermi distribution function for electrons within the left or right electrode is given by

$$f_{\mu_{L(R)}}(\varepsilon) = \left[1 + \exp\left(\frac{\varepsilon - \mu_{L(R)}}{k_BT}\right)\right]^{-1}.$$

We consider the transport properties of the three-site quantum wire when the electrochemical potentials μ_L and μ_R are associated with the left and right electrodes, respectively. It is equivalent to the case of applying a bias voltage $-V$ to the wire ($eV = \mu_L - \mu_R$). Since the spin degeneracy due to absence of the Coulomb interaction, the following formulas only give the single-spin electron transport properties without distinguishing the spin orientation. When we consider the case including the up and down spin, all results should be multiplied by 2.

The current flowing in the wire is equal to the current between the wire region and the left electrode. It can be obtain by substituting Keldysh Green's function eqs. (20a) and (20b) into eq. (10).[16–19]

$$I_\sigma(\mu_L, \mu_R) = \frac{e}{h}\int_{-\infty}^{+\infty} d\varepsilon(f_{\mu_L} - f_{\mu_R})\frac{4\Gamma^r_{L\sigma}\Gamma^r_{R\sigma}|t_{12\sigma}t_{23\sigma}|^2}{|B^r_\sigma|^2} \tag{24}$$

The corresponding nonnequilibrium conductance, therefore, is straightforwardly given by

$$G_\sigma(\mu_L, \mu_R) = \frac{I_\sigma(\mu_L, \mu_R)}{(\mu_L - \mu_R)/e} = \frac{1}{\mu_L - \mu_R} \times \frac{e^2}{h}\int_{-\infty}^{+\infty} d\varepsilon(f_{\mu_L} - f_{\mu_R})\frac{4\Gamma^r_{L\sigma}\Gamma^r_{R\sigma}|t_{12\sigma}t_{23\sigma}|^2}{|B^r_\sigma|^2}. \tag{25}$$

The general formula for calculating differential conductance (transmission coefficient) is shown as

$$g_\sigma(\mu_{L(R)}) = \lim_{\mu_L\to\mu_R}\frac{I_\sigma(\mu_L, \mu_R)}{(\mu_L - \mu_R)/e} = \frac{e^2}{h}\int_{-\infty}^{+\infty} d\varepsilon\left\{\frac{4\Gamma^r_{L\sigma}\Gamma^r_{R\sigma}|t_{12\sigma}t_{23\sigma}|^2}{|B^r_\sigma|^2}\left(\frac{1}{4k_BT}\frac{1}{\cosh^2\left(\frac{\varepsilon - \mu_{L(R)}}{2k_BT}\right)}\right)\right\}. \tag{26}$$

In particular, when temperature $T = 0$, eq. (26) reduces to

$$g_\sigma(\mu_{L(R)}) = \frac{e^2}{h}\frac{4\Gamma^r_{L\sigma}\Gamma^r_{R\sigma}|t_{12\sigma}t_{23\sigma}|^2}{|B^r_\sigma|^2}\Big|_{\varepsilon=\mu_{L(R)}}. \tag{27}$$

The electronic charges on the sites will be obtained by substituting Keldysh Green's function eqs. (23a)–(23c) for eq. (11).

$$\rho_{1\sigma,1\sigma}(\mu_L, \mu_R) = \frac{e}{\pi}\int_{-\infty}^{+\infty} d\varepsilon\left\{\frac{f_{\mu_L}\Gamma^r_{L\sigma}[(x_{2\sigma}x_{3\sigma} - |t_{23\sigma}|^2)^2 + (\Gamma^r_{R\sigma})^2x^2_{2\sigma}] + f_{\mu_R}\Gamma^r_{R\sigma}|t_{12\sigma}t_{23\sigma}|^2}{|B^r_\sigma|^2}\right\} \tag{28a}$$

$$\rho_{2\sigma,2\sigma}(\mu_L, \mu_R) = \frac{e}{\pi}\int_{-\infty}^{+\infty} d\varepsilon\left\{\frac{f_{\mu_L}\Gamma^r_{L\sigma}[x^2_{3\sigma} + (\Gamma^r_{R\sigma})^2]|t_{12\sigma}|^2 + f_{\mu_R}\Gamma^r_{R\sigma}[x^2_{1\sigma} + (\Gamma^r_{L\sigma})^2]|t_{23\sigma}|^2}{|B^r_\sigma|^2}\right\} \tag{28b}$$

$$\rho_{3\sigma,3\sigma}(\mu_L, \mu_R) = \frac{e}{\pi}\int_{-\infty}^{+\infty} d\varepsilon\left\{\frac{f_{\mu_L}\Gamma^r_{L\sigma}|t_{12\sigma}t_{23\sigma}|^2 + f_{\mu_R}\Gamma^r_{R\sigma}[(x_{1\sigma}x_{2\sigma} - |t_{12\sigma}|^2)^2 + (\Gamma^r_{L\sigma})^2x^2_{2\sigma}]}{|B^r_\sigma|^2}\right\} \tag{28c}$$

4. Numerical Results and Interpretations

In this section, we calculate the single-spin electron transport properties of the three-site quantum wire in some special cases using the formulas provided in the previous section, and give their physical interpretations. We assume that the transfer integrals $t_{12\sigma} = t_{23\sigma} = t$, and the tunnel combination integrals $V_{L,k\sigma} = V_{R,k\sigma} = V$. Furthermore, the DOS in the electrodes is $\nu_{L\sigma}(\varepsilon) = \nu_{R\sigma}(\varepsilon) = \nu$. Hence, the self-energies $\Gamma_{L\sigma}(\varepsilon) = \Gamma_{R\sigma}(\varepsilon) = \Gamma$. For simplicity, all of the energies are normalized by the transfer integral t, e.g., $\mu_{L(R)} \to \mu_{L(R)}/t$ and $k_BT \to k_BT/t$. We introduce the new parameters by the following definitions:

$$\gamma = \Gamma/t,\ y = \varepsilon/t,\ y_i = \varepsilon_{i\sigma}/t,\ i = 1, 2, 3$$

For computing the nonequilibrium transport properties using the formulas above, the integrals in eqs. (24)–(28) are replaced by Simpson's sums, and the mesh is taken to be typically $dy = d\varepsilon/t = 10^{-4}$. We present the numerical results as follows.

4.1 A uniform-ingredient wire when $T = 0\,K$

We assume that $k_BT = 0$ and the on site-energies $y_1 = y_2 = y_3 = y_0 = 0$. As the numerical results, differential conductance, which is identical to transmission coefficient, as a function of the electrochemical potential μ for several values of γ is illustrated in Fig. 2(a).

Differential conductance changes markedly when the value of γ crosses unity. It has three maximums at $\mu = 0$ and $\pm\sqrt{2}$ when $\gamma < 1$, whereas it has a single maximum at $\mu = 0$ when $\gamma > 1$. This change in the line shape can also be regarded as differential conductance as a function of gate voltage applied to the quantum wire. The parameter γ essentially represents the relative strength of the wire–electrode coupling and that of the site–site coupling within the wire. When $\gamma < 1$, the site–site coupling is stronger than that of the wire–electrode coupling, therefore, the whole system appears similar to a double-barriers structure, that is, the wire with multiple levels is pinched by the left and right wire–electrode barriers. The lines observed near the three maximums are the spectra of molecular levels of electrons within the wire. In this case, the maximum conductance is always equal to unity of quantum conductance. This finding implies that the electrons flow through the wire using these molecular levels and that resonant tunneling takes place.[7,20] In the opposite case, when $\gamma > 1$, the wire–electrode coupling is stronger than the site–site coupling, so that the barriers are located at the places of the site 1–site 2 and site 2–site 3 combinations and the intermediate part is only site 2. The observation of a single maximum means that only one level exists within site 2 and that resonant tunneling takes place. It can be considered a halfway state between the two cases discussed above when $\gamma = 1$. In general, with the increase in the number of sites in the wire, the space between the levels decreases. Consequently, when $\gamma < 1$, because the double-barrier structure is not changed, the site number of maximums will appear and the space between neighboring maximums decreases accompanied by a decrease in the space of the level. On the other hand, when $\gamma > 1$, the whole system becomes a multiple-barrier structure, and complex resonant peaks will appear. If the number of sites reaches an infinite large limit, instead of discrete levels, some continuous bands will be formed. It is different from the discrete case, in which the positions and values of resonant peaks are qualitatively determined by the DOS of the electronic bands and initial electrons occupation states.

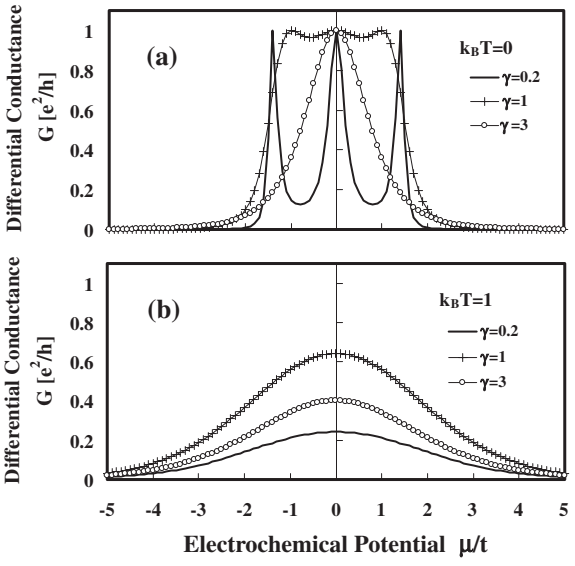

Fig. 2. Differential conductance (equivalent to transmission coefficient) of a uniform-ingredient wire as a function of electrochemical potential μ under conditions of different self-energies $\gamma = 0.2$, 1, and 3, calculated using eqs. (26) and (27). (a) When $k_BT = 0$ ($T = 0\,K$). (b) When $k_BT = 1$ ($T > 0\,K$). μ can also be regarded as incident electron energy. All of the energies are normalized by the transfer integral t, and the conductance unit is e^2/h.

Under the condition of a fixed $\mu_R = -5$, transport current as a function of the electrochemical potential μ_L for the same values of γ shown in Fig. 2(a) is illustrated in Fig. 3(a).

From the differential conductance line shape, it is obvious that the current line climbs rapidly when the differential conductance has a peak, while it shows a flat plateau when the differential conductance drops in a valley near zero. In Particular, it is remarkable that current increases intermittently with a step-shape when $\gamma < 1$. This phenomenon implies that conductance quantization takes place easily in this case. The saturation current shown in Fig. 3(a) can be expressed by eq. (29) shown below, which is obtained from eq. (24) with the limit of Fermi distribution function as $\mu_L \to \infty$, i.e., $\lim_{\mu_L \to \infty} f_{\mu_L}(\varepsilon) = 1$. The relationship between the saturated value and the parameter γ is also given by this equation. Actually, the saturation current can be estimated by the area enclosed by the differential conductance curve and the x-axis in Fig. 2(a) (note that $\mu_R = -5$), approximately 1.2 for $\gamma = 0.2$, 3.1 for $\gamma = 1$, and 1.9 for $\gamma = 3$.

$$I_{sat}(\mu_R) = \frac{e}{h}\int_{-\infty}^{+\infty} d\varepsilon (1 - f_{\mu_R}) \frac{4\Gamma^r_{L\sigma}\Gamma^r_{R\sigma}|t_{12\sigma}t_{23\sigma}|^2}{|B^r_\sigma|^2} \qquad (29)$$

Under the same conditions as those shown in Fig. 3(a), the total conductance as a function of the electrochemical potential difference between the two electrodes $\mu_L - \mu_R$, in proportion with the bias voltage, is illustrated in Fig. 4(a). The step-shape conductance appearing in the figure is what we call conductance quantization.

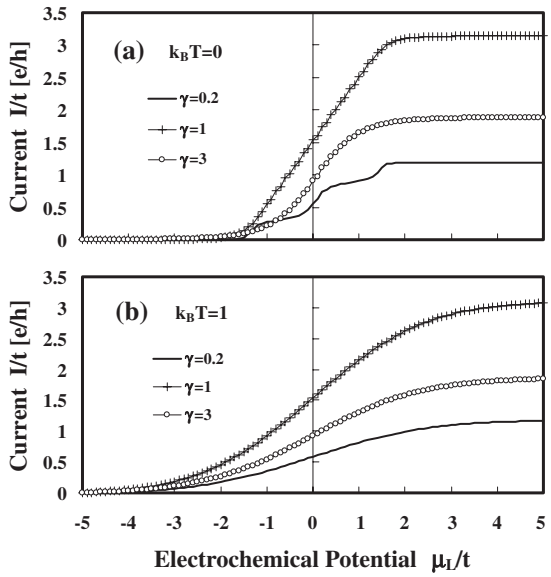

Fig. 3. Transport current of a uniform-ingredient wire as a function of electrochemical potential of the left electrode μ_L (electrochemical potential of the right electrode is fixed at $\mu_R = -5$) under conditions of different self energies $\gamma = 0.2$, 1, and 3, calculated using eq. (24). (a) When $k_BT = 0$ ($T = 0$ K). (b) When $k_BT = 1$ ($T > 0$ K). The bias voltage V applied to the wire can be expressed as $V = (\mu_L - \mu_R)/e$. All of the energies are normalized by the transfer integral t, and the current unit is et/h.

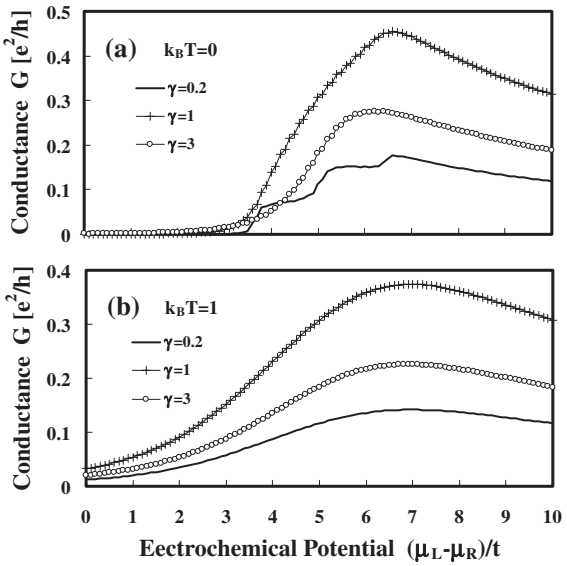

Fig. 4. Total conductance of a uniform-ingredient wire as a function of electrochemical potential of the left electrode μ_L (electrochemical potential of the right electrode is fixed at $\mu_R = -5$) under conditions of different self-energies $\gamma = 0.2$, 1, and 3, calculated using eq. (25). (a) When $k_BT = 0$ ($T = 0$ K). (b)When $k_BT = 1$ ($T > 0$ K). The bias voltage V applied to the wire can be expressed as $V = (\mu_L - \mu_R)/e$. All of the energies are normalized by the transfer integral t, and the conductance unit is e^2/h.

We next consider the change in charge distribution in the three sites with the increase in the electrochemical potential of the electrodes. Firstly, we suppose the electrochemical potential of the left electrode is equal to that of the right electrode ($\mu_L = \mu_R$), accordingly there is no current flowing in the wire. This corresponds to the case of combining the electrodes and wire that have different electrochemical potentials (The electrochemical potential of the wire is $\mu_W = 0$ here), and the initial charge barrier (Schottky barrier) can be investigate regardless of the Coulomb interaction. Usually, the work function of a material is identical to the electrochemical potential of the material. The charge distributions in the three sites as a function of μ for the same values of γ shown in Fig. 2(a) are illustrated in Figs. 5(a1), 5(b1), and 5(c1).

The charges in sites 1 and 3 are identical, and are different from that in site 2 because of the symmetric system. A distinct difference in charge distribution also appears when the value of γ crosses unity. When $\gamma < 1$, the wire can be observed as a molecular with levels of about $-\sqrt{2}$, 0, and $+\sqrt{2}$. For this reason, the charges in the sites are all zero (empty) when $\mu < -\sqrt{2}$ (the lowest level) and are all unity (full) when $\mu > +\sqrt{2}$ (the highest level), indicating that there are no barriers on the wire. In the intermediate area ($-\sqrt{2} < \mu < +\sqrt{2}$), the charges in the sites increase from 0 to 1. It is interesting that in the area of $-\sqrt{2} < \mu < 0$, the charge in site 2 increases more rapidly than those in sites 1 and 3, resulting in a plus-charge barrier at the boundary of the wire. Whereas in the area of $0 < \mu < +\sqrt{2}$, the reverse trend results in a minus-charge barrier at the boundary of the wire. This finding can be interpreted by the weights of the site orbits composing the molecular orbit according to detailed calculations. When $\gamma > 1$, sites 1 and 3 strongly combine with the electrodes, and site 2 is isolated by the site–site barrier to become a single site. For this reason, the charges in sites 1 and 3 increase slowly near the value of 0.5 because of the strong combinations of the electrodes, while the charge in site 2 vary from 0 to 1 similar to a single-level molecular. This results in the fact that in the area of $\mu < 0$, a minus-charge barrier will be formed at the boundary of the wire, whereas in the area of $\mu > 0$, a plus-charge barrier will be formed. When $\gamma = 1$, it is a halfway state between the two cases discussed above.

The process is dynamic when the electrochemical potential of the left electrode is greater than that of the left electrode, because current starts to flow in the wire, and the charge distributions in the sites in this case are essentially different from those in static case discussed above. Under the condition of a fixed μ_R which is similar to the condition in current analysis, the charge distributions in the three sites as a function of μ_L are illustrated in Figs. 6(a1), 6(b1), and 6(c1). When $\gamma < 1$, the charges in the sites show a trend similar to that in the static case except that the values of the charges are only one half of that in the static case owing to the existence of current. Of course the charge barrier at the boundary of the wire decreases accordingly. When $\gamma > 1$, the charge in site 2 shows a trend similar to that in the static case, while the charge in site 1 increases and charge of in site 2 shows almost no change. This results in charge accumulation in site 1 owing to the site–site barrier that prevents the charges in site 1 from flowing to site 2. The charges as well as the charge barrier also decrease owing to the existence of current.

4.2 A uniform-ingredient wire when $T > 0$ K

The quantum transport properties are affected by temperature owing to the Coulomb interaction or electron–phonon

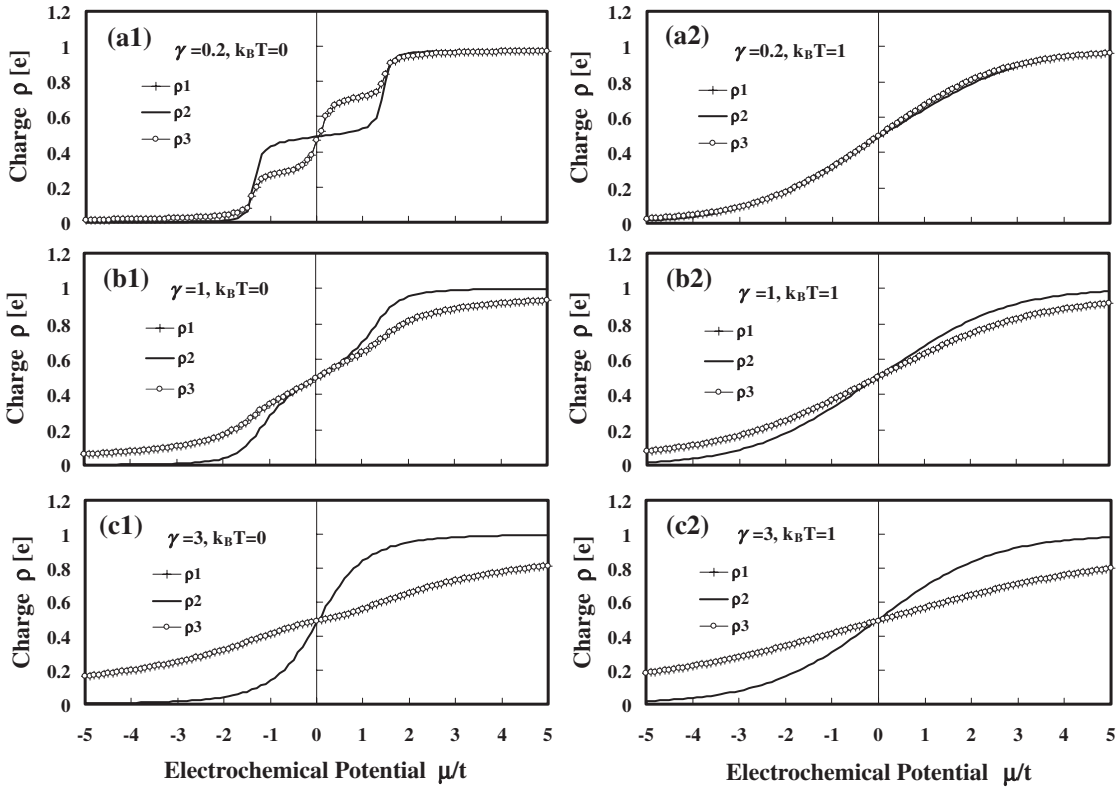

Fig. 5. Electronic charges in the three sites of a uniform-ingredient wire as a function of electrochemical potential μ, supposing that the electrochemical potential of the left electrode is equal to that of the right electrode ($\mu = \mu_L = \mu_R$) under conditions of different self-energies, calculated using eqs. (28a)–(28c). (a1) When $\gamma = 0.2$, $k_BT = 0$ ($T = 0$ K). (b1) When $\gamma = 1$, $k_BT = 0$ ($T = 0$ K). (c1) When $\gamma = 3$, $k_BT = 0$ ($T = 0$ K). (a2) When $\gamma = 0.2$, $k_BT = 1$ ($T > 0$ K). (b2) When $\gamma = 1$, $k_BT = 1$ ($T > 0$ K). (c2) When $\gamma = 3$, $k_BT = 1$ ($T > 0$ K). Since the bias voltage V [$= (\mu_L - \mu_R)/e$] applied to the wire is equal to zero, there is no current flowing in the wire. $\rho 1$, $\rho 2$, and $\rho 3$ denote the charges in sites 1, 2, and 3, respectively. All of the energies are normalized by the transfer integral t, and the charge unit is the electron charge e.

interaction, e.g., the Kondo effect. Similarly, in the case of noninteraction, when the thermal energy k_BT is comparable to the transfer energy between the sites of the wire or between the wire and electrodes, the temperature dependence can be easily observed.

We assume $k_BT = 1$ which is equal to the energy unit of the transfer energy t. Under the same conditions described in §4.1 except for $k_BT = 1$, the differential conductance, transport current, total conductance, and electronic charges in the sites of the wire as a function of the electrochemical potentials of the electrodes are illustrated in Figs. 2(b), 3(b), 4(b), 5(a2), 5(b2), 5(c2), 6(a2), 6(b2), and 6(c2), respectively.

A common phenomenon is that the line shapes of the transport characteristics in the figures do not change markedly and all become smoother than those at $T = 0$ K. In particular, when $\gamma < 1$, we almost cannot distinguish the peak values of the differential conductance shown in Fig. 2(b), or the step-shape of the current, conductance, and electronic charges shown in the Figs. 3(b), 4(b), 5(a2), 5(b2), 6(a2), and 6(b2) as the case of $k_BT = 0$. It is essential that with the increase in temperature, the interference of transport electron waves is destroyed gradually by thermal fluctuations, leading to that a coherent transport in the wire becomes an incoherent transport.

4.3 Wire containing impurities when $T = 0$ K

We consider that the on-site energy in site 2 at the center of the wire is higher or lower than those the in remaining sites, which shows that there is an impurity component (site 2) in the wire, and present the transport properties of the wire.

We assume that the on-site energies of the sites in the wire are $y_1 = y_3 = y_0$, $y_2 = y_0 - \Delta y$, where $\Delta y = 1$ and -1 represent the higher and lower levels in site 2, respectively. The absolute values of Δy are equivalent to the energy unit (the transfer energy t). Under the same conditions as those described in the §4.1, the differential conductance, transport current, total conductance, and electronic charges in the sites of the wire as a function of the electrochemical potentials of the electrodes are illustrated in Figs. 7–11, respectively.

Besides the difference in the positions of the peak values of differential conductance, or the change points of the step-shape of current, conductance, and electronic charges, the line shapes of the transport characteristics in the figures are similar to those described in §4.1. As indicated in §4.1, because the on-site energy in site 2 is changed, the spectra of molecular levels of the wire are also changed accordingly. When $\gamma < 1$, the molecular levels shift to the new positions of $y = -1, 0, 2$ and $-2, 0, 1$ for $\Delta y = 1$ and -1, respectively. On the other hand, when $\gamma > 1$, the new position is $y = 1$ and -1 for $\Delta y = 1$ and -1, respectively. This finding directly results in changes in the transport properties. On the other hand, the increasing rates of site charges as well as the charge barrier in the wire are also different from those described in §4.1, probably owing to the changes in the weights of the site orbits composing the molecular orbit.

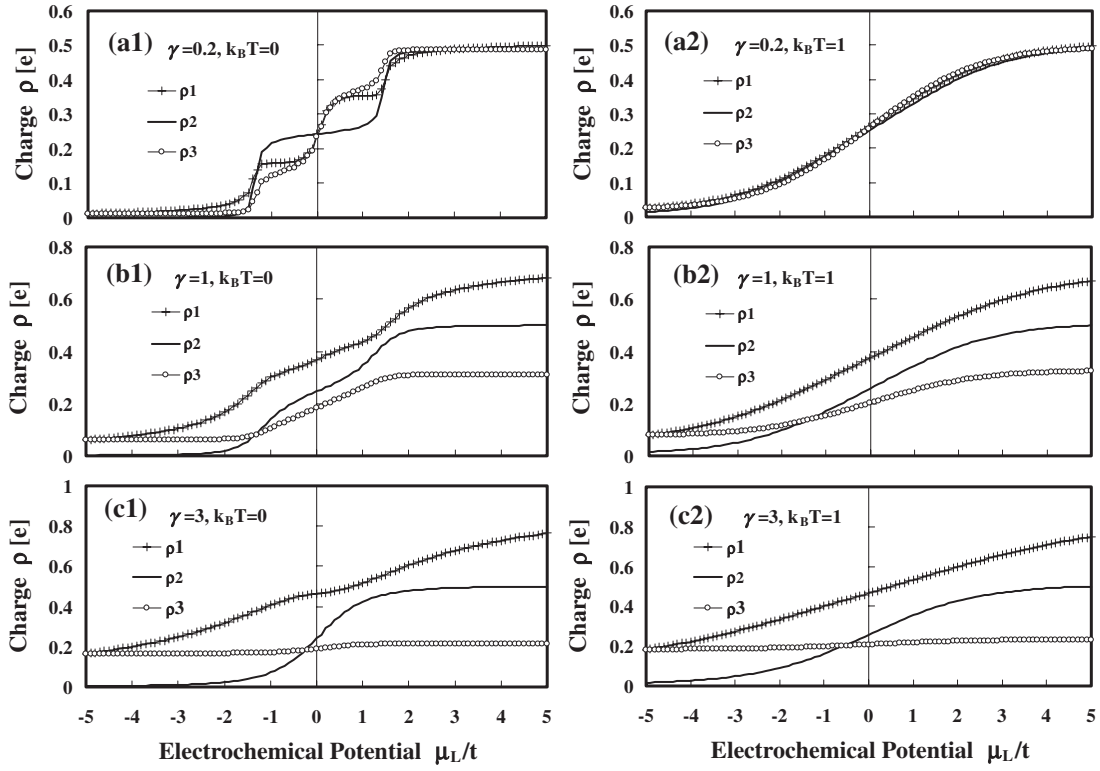

Fig. 6. Electronic charges in the three sites of a uniform-ingredient wire as a function of electrochemical potential of the left electrode μ_L (electrochemical potential of the right electrode is fixed at $\mu_R = -5$) under conditions of different self-energies, calculated using eqs. (28a)–(28c). (a1) When $\gamma = 0.2$, $k_BT = 0$ ($T = 0$ K). (b1) When $\gamma = 1$, $k_BT = 0$ ($T = 0$ K). (c1) When $\gamma = 3$, $k_BT = 0$ ($T = 0$ K). (a2) When $\gamma = 0.2$, $k_BT = 1$ ($T > 0$ K). (b2) When $\gamma = 1$, $k_BT = 1$ ($T > 0$ K). (c2) When $\gamma = 3$, $k_BT = 1$ ($T > 0$ K). The bias voltage V applied to the wire can be expressed as $V = (\mu_L - \mu_R)/e$. $\rho 1$, $\rho 2$, and $\rho 3$ denote the charges in sites 1, 2, and 3, respectively. All of the energies are normalized by the transfer integral t, and the charge unit is the electron charge e.

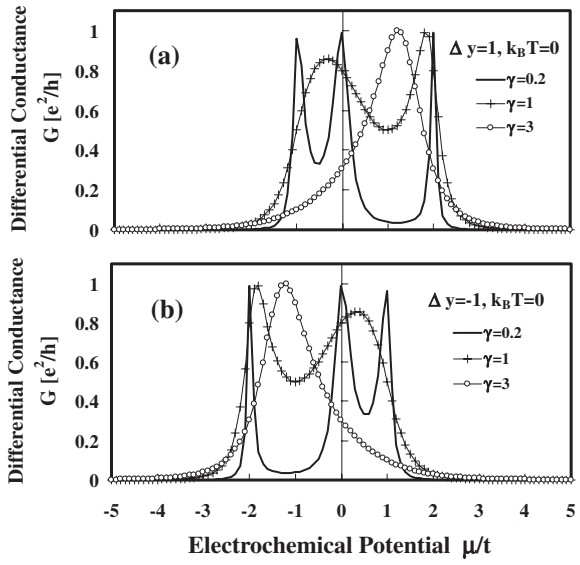

Fig. 7. Differential conductance (equivalent to transmission coefficient) of a wire containing impurities as a function of electrochemical potential μ under conditions of different self-energies $\gamma = 0.2$, 1, and 3 when $k_BT = 0$ ($T = 0$ K), calculated using eq. (27). (a) When $\Delta y = 1$. (b) When $\Delta y = -1$. μ also can be regarded as incident electron energy. All of the energies are normalized by the transfer integral t, and the conductance unit is e^2/h.

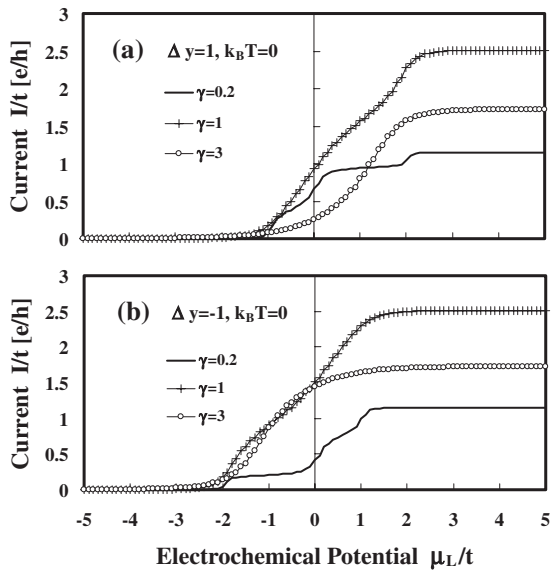

Fig. 8. Transport current of a wire containing impurities as a function of electrochemical potential of the left electrode μ_L (electrochemical potential of the right electrode is fixed at $\mu_R = -5$) under conditions of different self-energies $\gamma = 0.2$, 1, and 3 when $k_BT = 0$ ($T = 0$ K), calculated using eq. (24). (a) When $\Delta y = 1$. (b) When $\Delta y = -1$. The bias voltage V applied to the wire can be expressed as $V = (\mu_L - \mu_R)/e$. All of the energies are normalized by the transfer integral t, and the current unit is et/h.

5. Conclusions and Discussion

On the basis of the Keldysh formalism, we derived some rigorous formulas for differential conductance (transmission coefficient), total conductance, nonequilibrium current, and electronic charges using the simplest model of a three-site quantum wire. Similar processes can be carried out for larger

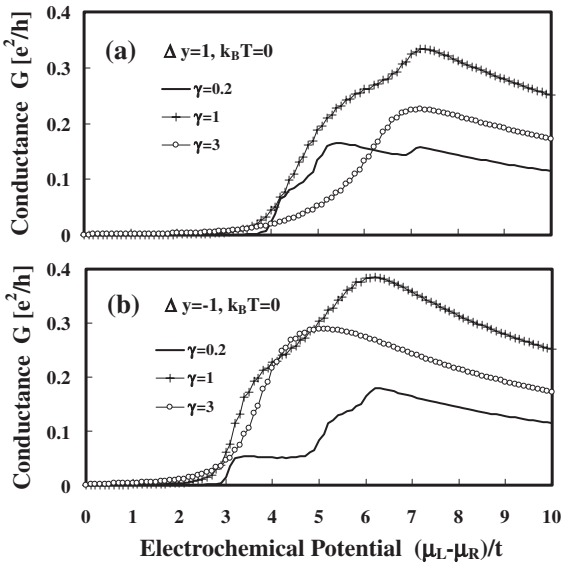

Fig. 9. Total conductance of a wire containing impurities as a function of electrochemical potential of the left electrode μ_L (electrochemical potential of the right electrode is fixed at $\mu_R = -5$) under conditions of different self-energies $\gamma = 0.2$, 1, and 3 when $k_BT = 0$ ($T = 0$ K), calculated using eq. (26). (a) When $\Delta y = 1$. (b) When $\Delta y = -1$. The bias voltage V applied to the wire can be expressed as $V = (\mu_L - \mu_R)/e$. All of the energies are normalized by the transfer integral t, and the conductance unit is e^2/h.

numbers of sites and multiple levels. Within a Hartree–Fock approximation level, one can include the effects of interaction in a straightforward manner.

Using these formulas, we executed direct calculations of quantum wire transport properties in some special occasions. For a uniform-ingredient wire, at $T = 0$ K, if the site–site coupling in wire is stronger than the wire–electrode coupling ($\gamma < 1$), the multiple maximums appear in the differential conductance characteristics and the step-shape appears in the current curves, indicating that the resonant tunneling transport takes place and the phenomenon of conductance quantization can be easily observed. On the other hand, if the wire–electrode coupling is stronger than the site–site coupling in the wire ($\gamma > 1$), the quantum effects on transport properties described above will disappear gradually with the increase in γ. The charge distributions on the three sites of the wire are calculated in the no-current-flowing case ($\mu_L = \mu_R$) and the current flowing-case ($\mu_L > \mu_R$). Furthermore, we discussed the characteristics of the charge barrier (Schottky barrier) regardless of the Coulomb interaction. When $T > 0$ K, we calculated the case of $k_BT = 1$. The results show a common phenomenon that the line shapes of the transport characteristics do not change markedly and all become smoother than those at $T = 0$ K owing to thermal fluctuations. For a wire containing impurities, the line shapes of the transport properties are similar to those in the uniform-ingredient case but the positions of the characteristic points (e.g., peak values, etc.) are changed

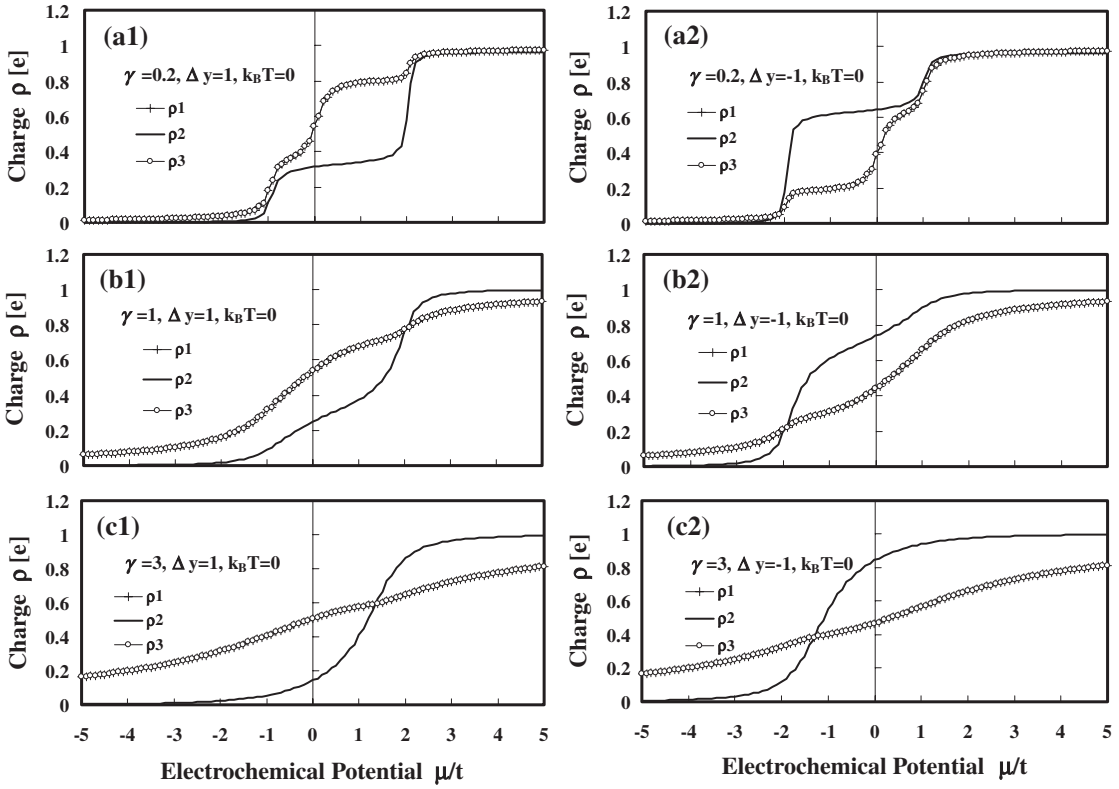

Fig. 10. Electronic charges in the three sites of a wire containing impurities as a function of electrochemical potential μ, supposing that the electrochemical potential of the left electrode is equal to that of the right electrode ($\mu = \mu_L = \mu_R$) under conditions of different self-energies when $k_BT = 0$ ($T = 0$ K), calculated using eqs. (28a)–(28c). (a1) When $\gamma = 0.2$, $\Delta y = 1$. (b1) When $\gamma = 1$, $\Delta y = 1$. (c1) When $\gamma = 3$, $\Delta y = 1$. (a2) When $\gamma = 0.2$, $\Delta y = -1$. (b2) When $\gamma = 1$, $\Delta y = -1$. (c2) When $\gamma = 3$, $\Delta y = -1$. Since the bias voltage V [$= (\mu_L - \mu_R)/e$] applied to the wire is equal to zero, there is no current flowing in the wire. $\rho 1$, $\rho 2$, and $\rho 3$ denote the charges in sites 1, 2, and 3, respectively. All of the energies are normalized by the transfer integral t, and the charge unit is the electron charge e.

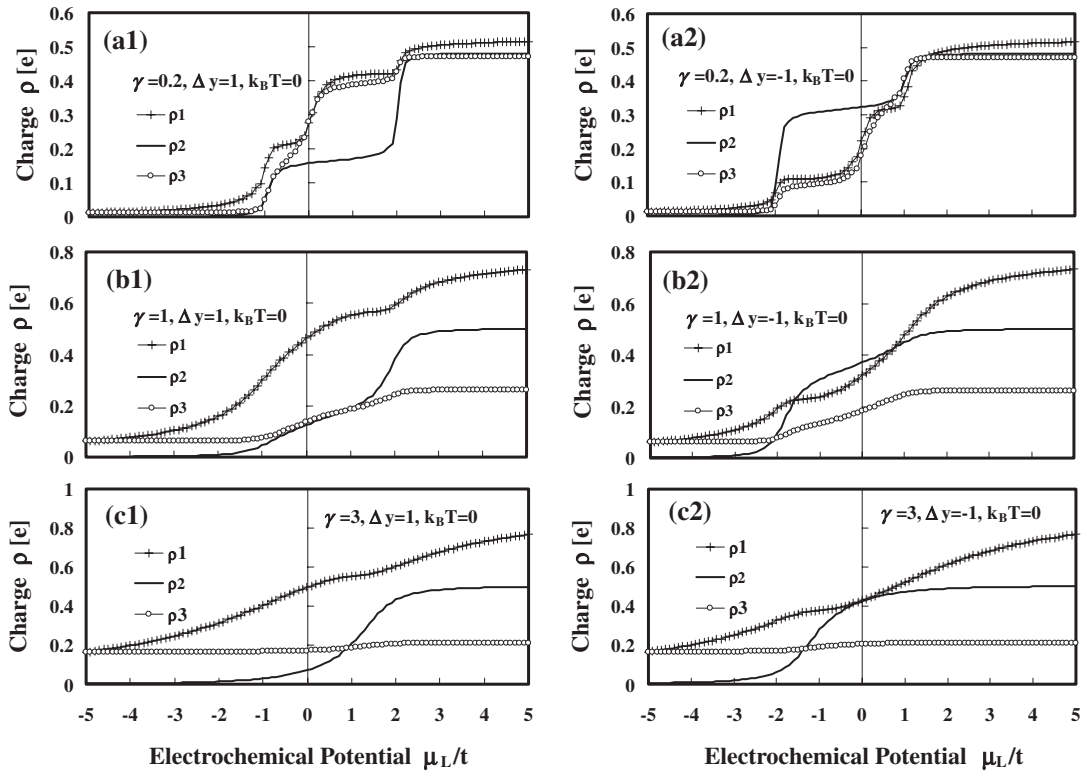

Fig. 11. Electronic charges in the three sites of a wire containing impurities as a function of electrochemical potential of the left electrode μ_L (electrochemical potential of the right electrode is fixed at $\mu_R = -5$) under conditions of different self-energies when $k_BT = 0$ ($T = 0$ K), calculated by eqs. (28a)–(28c). (a1) When $\gamma = 0.2$, $\Delta y = 1$. (b1) When $\gamma = 1$, $\Delta y = 1$. (c1) When $\gamma = 3$, $\Delta y = 1$. (a2) When $\gamma = 0.2$, $\Delta y = -1$. (b2) When $\gamma = 1$, $\Delta y = -1$. (c2) When $\gamma = 3$, $\Delta y = -1$. The bias voltage V applied to the wire can be expressed as $V = (\mu_L - \mu_R)/e$. $\rho 1$, $\rho 2$, and $\rho 3$ denote the charges in sites 1, 2, and 3, respectively. All of the energies are normalized by the transfer integral t, and the charge unit is the electron charge e.

because of the change in system electronic state. Accordingly, we should stress in particular that, besides the quantum wire itself, the properties of the electrodes, e.g., the DOS and the combinations between the wire and the electrodes, will strongly affect the transport features of the system. It can be considered that the numerical results presented in this paper provided a qualitative evaluation available for real quantum wires, for example, the semiconductor quantum wires such as silicon nanowires and carbon nanotubes.

Acknowledgement

The authors would like to acknowledge Dr. M. Okamoto, Mechanical Research Laboratory, Hitachi Ltd., for providing useful information about the first-principles calculations on quantum nanowires.

1) S. Iijima and T. Ichihashi: Nature (London) **363** (1993) 603.
2) D. S. Bethune, C. H. Kiang, M. S. de Vries, G. Gorman, R. Savoy, J. Vazquez, and R. Beyers: Nature (London) **363** (1993) 605.
3) X. Duan, Y. Huang, Y. Cui, J. Wang, and C. M. Lieber: Nature (London) **409** (2001) 66.
4) D. D. D. Ma, C. S. Lee, F. C. K. Au, S. Y. Tong, and S. T. Lee: Science **299** (2003) 1874.
5) Y. Cui, L. J. Lauhon, M. S. Gudiksen, J. Wang, and C. M. Lieber: Appl. Phys. Lett. **78** (2001) 2214.
6) S. Nonoyama and A. Oguri: Phys. Rev. B **57** (1998) 8797.
7) R. Tamura: Phys. Rev. B **67** (2003) 121408.
8) J.-L. Mozos, C. C. Wan, G. Taraschi, J. Wang, and H. Guo: Phys. Rev. B **56** (1997) R4351.
9) U. Landman, R. N. Barnett, A. G. Scherbakov, and P. Avouris: Phys. Rev. Lett. **85** (2000) 1958.
10) M. Brandbyge, J. Mozos, P. Ordejon, J. Taylor, and K. Stokbro: Phys. Rev. B **65** (2002) 165401.
11) J. Schwinger: J. Math. Phys. **2** (1961) 407.
12) L. V. Keldysh: Sov. Phys. JETP **20** (1965) 1018.
13) C. Caroli, R. Combescot, P. Nozieres, and D. Saint-James: J. Phys. C **4** (1971) 916.
14) L. D. Landau and E. M. Lifshitz: *Statistical Physics Part 2* (Pergamon Press, New York, 1965) Course of Theoretical Physics, Vol. 9.
15) L. D. Landau and E. M. Lifshitz: *Physical Kinetics* (Pergamon Press, New York, 1965) Course of Theoretical Physics, Vol. 10.
16) Y. Meir and N. S. Wingreen: Phys. Rev. Lett. **68** (1992) 2512.
17) S. Hershfield, J. H. Davies, and J. W. Wilkins: Phys. Rev. B **46** (1992) 7046.
18) Y. Meir, N. S. Wingreen, and P. A. Lee: Phys. Rev. Lett. **66** (1991) 3048.
19) S. Datta: *Electronic Transport in Mesoscopic Systems* (Cambridge University Press, Cambridge, U.K., 1995).
20) H. Mizuta and T. Tanoue: *The Physics and Applications of Resonant Tunneling Diode* (Cambridge University Press, Cambridge, U.K., 1995).